ISSN 0915-633X

NATIONAL INSTITUTE FOR FUSION SCIENCE

Cuspher, A Combined Confinement System

T. Ohkawa and H. Ohkawa

(Received - Feb. 12, 1996)

NIFS-412 Apr. 1996

RESEARCH REPORT
NIFS Series

NAGOYA, JAPAN

Cuspher, A Combined Confinement System

Tihiro Ohkawa
National Institute for Fusion Science
and
University of California at San Diego

Hana Ohkawa
Plasma Fusion Center, Massachusetts Institute of Technology

Abstract

Cuspher is a magnetic confinement system which combines a closed [spheromak] and an open [cusp] system. The open system surrounds the closed system that provides a plasma reservoir. The closed system is assumed to have gross mhd stability but is not required to have plasma particle and energy confinement. The overall confinement is determined by the convective plasma loss from the open system and the volume of the closed system. The fusion condition may be attained in a relatively modest size device.

Keywords: combined confinement system, open system, closed system, cusp, spheromak, convective loss

[1] Introduction

The concept of the combined confinement system has been discussed previously.[1] Nested closed magnetic flux surfaces are surrounded by open magnetic lines. Because the plasma loss channels in the closed and the open system are in series, the overall confinement time τ is given by

$$\tau = \tau_c + \tau_o (1 + V_c / V_o) \qquad (1)$$

where V is the volume and the subscripts c and o denote the closed and the open systems. If the volume ratio V_c / V_o is large enough, the overall confinement time is sufficient to achieve fusion conditions even at the limit of $\tau_c \rightarrow 0$.

The separatrix surface which devides the closed and the open regions may or may not have the null of the magnetic field. In the former case, the plasma loss is cusp-like and in the latter case the loss is mirror-like. Since the line cusp loss is much larger than the point cusp loss, the prefered closed systems are tori with aspect ratio of unity, an example being a spheromak.

We examine the confinement characteristics of Cuspher - spheromak surrounded by cusp - in this report. The basic assumptions are [1] the spheromak is mhd stable, [2] the confinement time of the spheromak is nil and [3] the loss from the open system is convective. In the following sections, we discuss the configuration, the ion orbit, the cusp and the mirror losses, the start up and the device size for fusion.

[2] Configuration

The magnetic configuration consists of [A] spheromak region, [B] cusp region, [C] solenoid region and [D] expansion region as shown in Fig. 1. The spheromak acts as a reservoir of the plasma and it is assumed that the spheromak confinement time is much shorter than the confinement time of the open system. The plasma pressure is uniform inside the spheromak and it is a force free configuration. Region [B] is where the cusp and the mirror losses occur. The role of the solenoid region is to constrict the magnetic flux lines for reducing the cusp loss. Region [D] is to dispose the escaping plasma in such a way that the cold secondary particles cannot stream back into the confinement region.

[3] Ion orbit

The magnetic configuration is axisymmetric and the poloidal magnetic field can be derived from the flux function Ψ,

$$\left.\begin{aligned} B_r &= -[1/r]\,\partial\Psi/\partial z \\ B_z &= [1/r]\,\partial\Psi/\partial r \end{aligned}\right\} \qquad (2)$$

The seperatrix is the surface with $\Psi = 0$, which separates the spheromak region $\Psi < 0$ and the open flux line region $\Psi > 0$.

The azimuthal canonical anglar momentum P_θ is a constant of motion,

$$P_\theta = m\,r\,v_\theta + e\Psi \qquad (3)$$

where m and v are the ion mass and velocity. We examine the ion orbits near the seperatrix to find the relative positions of the orbits at the median plane of the spheromak and near the axis [r = 0] in the open line region.

The ions with $P_\theta = 0$ intersect the seperatrix at the median plane with $v_\theta = 0$. In the open line region the orbits go through the axis [r = 0] and the maximum radius of the orbit is twice the gyro-radius. These orbits pass through the null of the magnetic field and the magnetic moment is not an adiabatic constant.

The ions just outside of the seperatrix with the orbits tangent to the seperatrix have $P_\theta = m r_s v_\theta > 0$, where r_s is the radius of the spheromak. Away from the spheromak the guiding centers follow approximately the flux lines with $\Psi = m r_s v_\theta / e$. The radial position of the flux line is roughly the geometrical mean of the spheromak radius and the gyro-radius. The magnetic field on these orbits is finite and the magnetic moment is an adiabatic constant.

Similarly the ions just inside the spheromak with the orbits tangent to the seperatrix have $P_\theta = m r_s v_\theta < 0$. The radial position of the guiding center at the inboard side of the spheromak is roughly the geometrical mean of the spheromak radius and the gyro-radius. The magnetic moment is an adiabatic constant.

[4] Cusp and mirror losses

The ions just inside the spheromak will get on to the orbits $P_\theta = 0$ through the ion-ion collisions. Since magnetic moment is not constant, the ions are lost through the point cusp along the axis. The further collisions will take them to the orbits with $P_\theta > 0$. These ions will be mirror confined between the strong field regions produced by the solenoids. The mirror confinement time is of the order of the ion-ion collision time and the ions will be lost before they diffuse radially much further. As a result, the mirror confined orbits are limited to $0 < P_\theta < m r_s v_\theta$.

We estimate the cusp loss L_c by assuming that the plasma flows out at the ion thermal velocity through the holes determined by the magnetic field strength in the solenoid, namely

$$L_c = 2\, n v_i\, 4\pi\, \rho^{*2}\, \alpha \qquad (4)$$

where n is the plasma density, v_i is the ion thermal velocity, α is a numerical constant to be determined by more elaborate calculation of the hole size, ρ is the gyro-radius and *denotes the quantity in the solenoid region. Numerically, the cusp loss is given by

$$L_c \simeq \frac{\alpha\, n}{B^{*2}} \left(\frac{T_i}{e}\right)^{\frac{3}{2}} \times 10^{-2} \qquad (5)$$

The mirror loss L_m is given by

$$L_m = V_m\, n\, \nu_{ii}\, f\,(B^*/B_s) \qquad (6)$$

where V_m is the volume of the mirror region, ν_{ii} is the ion-ion collision frequency and f is a function of the mirror ratio.

If the thickness of the mirror plasma at the median plane is $\Delta\, r_s$ the mirror region is enclosed by the flux lines with $\Psi = B_s\, r_s\, \Delta r_s$. A rough estimate of the volume can be obtained by assuming that the length of the mirror region in the axial direction is $3r_s$ and the average magnetic field in the region is B_s. We obtain

$$V_m = 6\pi\, r_s^2\, \Delta\, r_s g \tag{7}$$

where g is a numerical factor to be calculated for the actual magnetic field distribution.

The considerations of the ion orbit and the mirror loss indicate that Δr_s is about an ion gyro-radius. However the steep pressure gradient thus created may make the ballooning mode unstable. The stability condition for the ballooning mode is given by

$$\Delta r_s \geq \frac{1}{2}\left(\frac{l}{\pi}\right)^2 \frac{\beta_s}{r_s} \tag{8}$$

where l is the length of the bad curvature region and

$$\beta_s = \frac{4\mu_0\, n\, T_i}{B_s^2} \tag{9}$$

By using a rough estimate for l given by

$$l \sim r_s\, (\pi / 2) \tag{10}$$

we obtain

$$\Delta r_s \geq r_s\, \beta_s / 8 \tag{11}$$

In calculating the mirror loss, we should take the larger of two, the gyro-radius or the ballooning limit as Δr_s. However we design a device in such a way that they are equal at the final temperature. The condition that they are equal is given by

$$n = 2.1 \times 10^{21} \left(\frac{T_i}{e}\right)^{-\frac{1}{2}} \frac{B_s}{r_s} \tag{12}$$

At lower temperatures with this design, the gyro-radius is larger than Δr_s determined from the ballooning stability condition for a given density. By taking the gyro-radius as the thickness the ballooning stability is assured up to the final temperature. The mirror loss becomes

$$L_m = 1.4 \times 10^{-15}\, fg \frac{n^2 r_s^2}{B_s}\left(\frac{T_i}{e}\right)^{-1} \tag{13}$$

We assume that the cusp loss and the mirror loss are in parallel and the overall confinement time is given by

$$\tau^{-1} = 2.7 \times 10^{-3}\left(\frac{\alpha}{B^{*2} r_s^3}\right)\left(\frac{T_i}{e}\right)^{\frac{3}{2}} + 4.5 \times 10^{-16}\left(\frac{nfg}{r_s B_s}\right)\left(\frac{T_i}{e}\right)^{-1} \tag{14}$$

The cusp loss scales as $T_i^{\,3/2}$ whereas the mirror loss scales nT_i^{-1}. The optimum is where the cusp and the mirror losses are equal,

$$n = 6.0 \times 10^{12}\left(\frac{B_s}{B^{*2} r_s^2}\right)\left(\frac{\alpha}{f g}\right)\left(\frac{T_i}{e}\right)^{\frac{5}{2}} \tag{15}$$

The optimal temperature is obtained by combining the above equation and the ballooning condition eq (12),

$$\left(\frac{T_i}{e}\right)^3 = 3.5 \times 10^8\left(\frac{f g}{\alpha}\right) B^{*2} r_s \tag{16}$$

and the corresponding density becomes

$$n = 7.9 \times 10^{19} B_s\left(\frac{\alpha}{fg}\right)^{1/6} r_s^{(-7/6)}\, B^{*\,(-1/3)} \tag{17}$$

The confinement figure of merit [$n\tau$] using the temperature and the density given by eq.(16) and eq(17) becomes

$$(n\tau)^{-1} = 1.3 \times 10^{-18}\, (fg)^{2/3}\, \alpha^{1/3}\, r_s^{4/3}\, B_s^{-1}\, B^{*(-2/3)} \tag{18}$$

By choosing $f \sim g \sim \alpha \sim 1$, $r_s = 3$m, $B_s = 3$T and $B^* = 30$T, the Lawson condition $n\tau = 10^{20}$ is obtained at $n = 2.0 \times 0^{19}\text{m}^{-3}$ and $T_i = 10^4$eV. The stored plasma energy is 11MJ and the heating power to maintain the steady state is 2.2MW.

[5] Start up

The spheromak must be created before it can be heated and maintained. A coil and a pair of electrodes are placed between the solenoids as shown in Fig.2. The time dependence of the currents in the solenoid, the coil and between the electrodes are shown in Fig.3.

The field of the solenoids is time independent. The time sequence of the coil current is similar to that in a field reversed configuration [FRC]. Prior to $t = \tau_1$ the current is reverse biased. Between t_1 and t_2, the current is switched to positive. The discharge is initiated and some of the poloidal flux is trapped to form closed lines. After t_2, the coil current is time independent.

The current between the electrodes is for producing the toroidal magnetic field or equivalently for injection of the helicity. It is on only between t_1 and t_2. It may be better to locate the electrodes radially outward as shown in Fig.2 as alternate positions. The electrodes are powered first in this case before the reversal of the coil current. The current flows along the field lines produced by the bias current in the coil. The coil current is switched after the plasma is produced by the current between the electrodes. The poloidal flux may be trapped better this way.

Immediately after the formation of the spheromak, the heating and the fueling must commence. At low temperatures the mirror loss dominates over the cusp loss and is proportional to $n^2 T_i^{-1}$. Because of the steeper dependence on density and the milder dependence on temperature, a modest beam fueling will keep the density in a narrow range almost independent of the temperature.

The heating power P should be high enough so that the temperature increases in much shorter time than the electromagnetic skin time of the spheromak. The condition is given by

$$P \gg 3\, n\, T_i V_c \left(\frac{1}{\tau} + \frac{1}{\mu_0 \sigma r_s^2} \right) \qquad (19)$$

where σ is Spitzer conductivity. The mirror confinement time is much shorter than the skin time even at low temperatures and the above condition means simply that the heating power must be significantly higher than the heating power to maintain the steady state.

After the electron temperature is raised sufficiently the current drive is initiated to maintain the steady state. Since the preferred density is relatively low, LHCD [Lower hybrid current drive] is a possibility.

[6] Discussion

According to the simple analysis described above, Cuspher has a possibility of reaching the fusion condition in a relatively modest scaled device. It gives us further motivation to examine the assumptions more carefully.

The crucial assumption is the gross stability of the spheromak especially against the modes with small azimuthal mode numbers. The tilt and the sideway shift are dangerous modes. In a sense, the spheromak is acting as a mhd anchor for the mirror configuration and the stability of the entire system must be confirmed by mhd analysis. It may become necessary to add the multipolar external field for stability.

The loss from the open system is assumed to be convective. The secondary particles; electrons, ions and neutrals from the wall where the field lines terminate must be controlled. The conduction cooling due to the secondary electrons and the ion cooling by charge exchange must be minimized as in any open systems. The more accurate estimate of the hole size of the cusp loss and the volume of the mirror region is needed. The size of the fusion device depends critically on the loss rate.

The assumption of the total absence of the confinement in the closed system may be too pessimistic. If there is some confinement, it helps to relax the ballooning requirement at the edge as well as the reduction of the plasma loss. Also the fusion products, namely α- particles, are produced at the center of the closed region and their orbits will be initially contained within closed region.

Cuspher retains the attractive attributes of the open systems, such as ease of impurity control and ash removal, small thermal load at the plasma exhaust and the absence of the toroidal components. When theoretical calculations and experimental tests confirm the stability and the confinement improvement over the simple open systems, it will become one of the candidate for attractive fusion reactors.

Reference

[1] T. Ohkawa, "*Combined Confinement System Applied to Tokamaks*", Kakuyugokenkyu **56**, (1986) 274

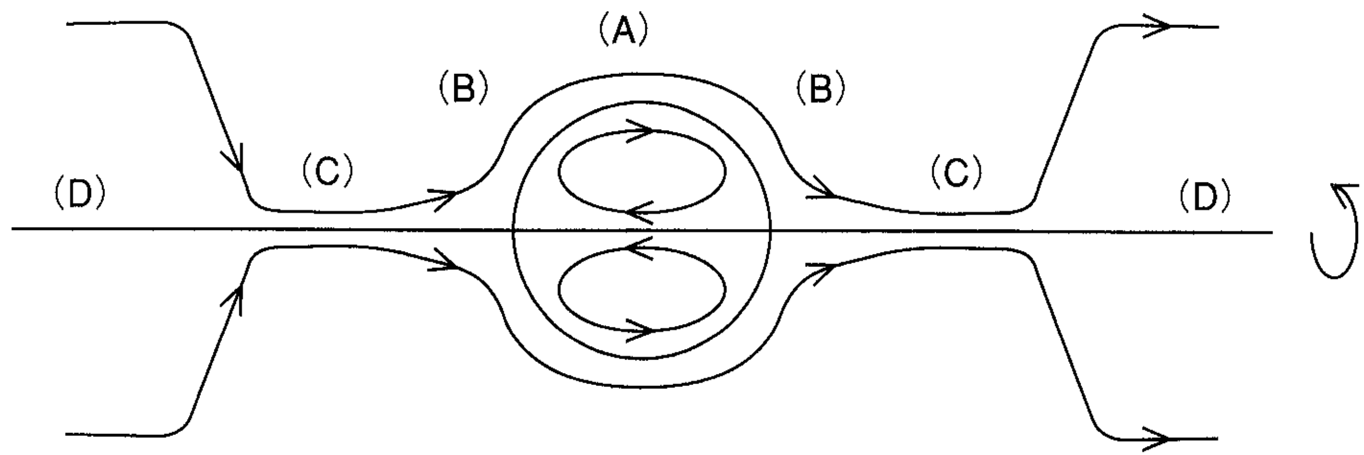

Fig.1 Cuspher configuration

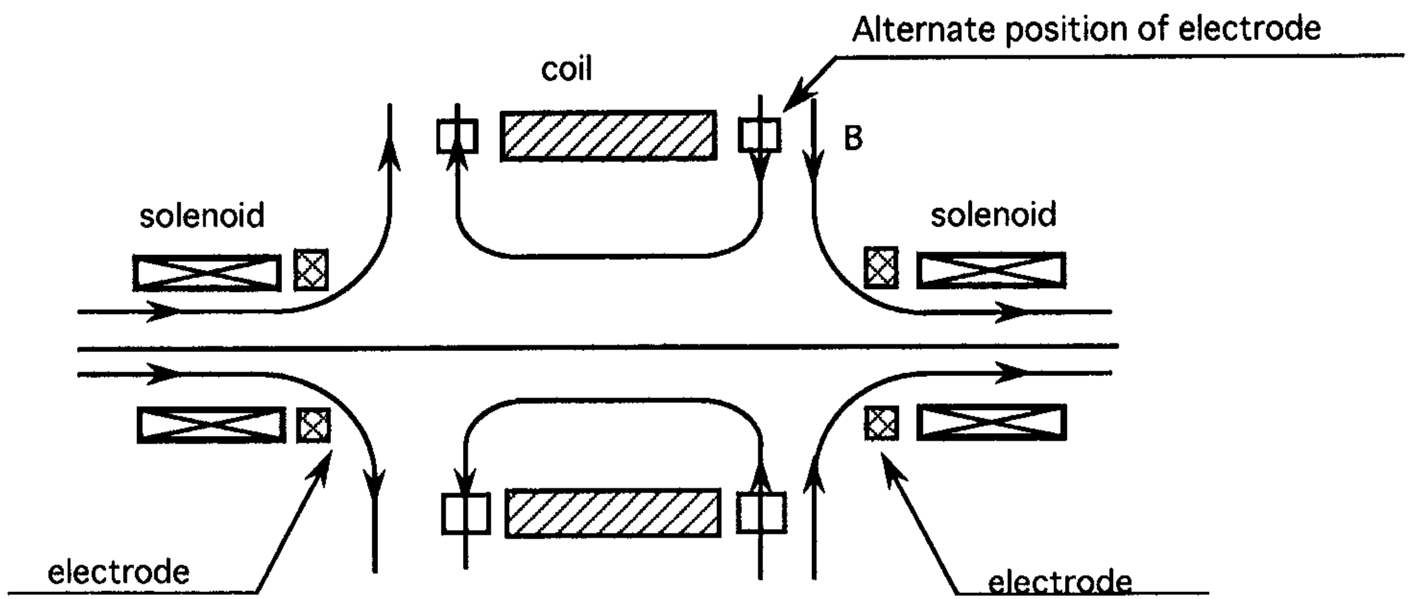

Fig.2 Start up arrangement

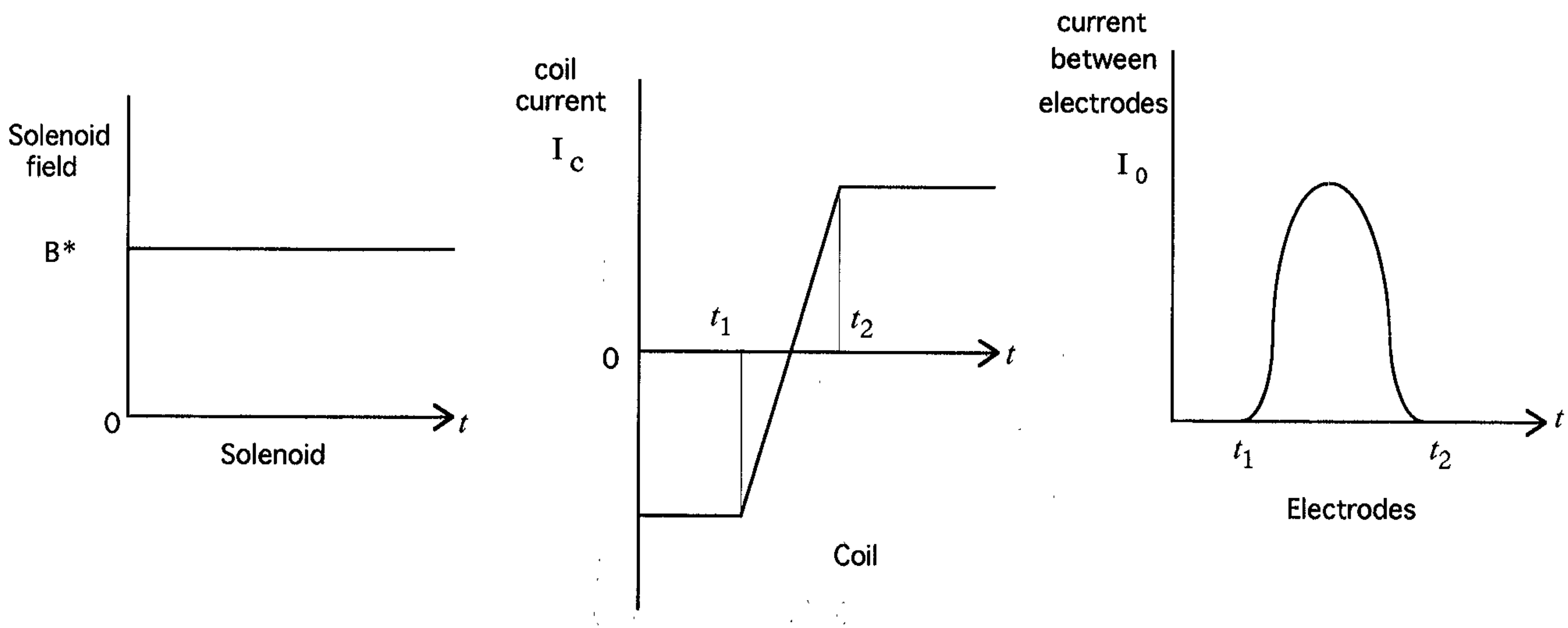

Fig.3 Time sequence of currents

Recent Issues of NIFS Series

NIFS-364 H. Sugama and W. Horton
Entropy Production and Onsager Symmetry in Neoclassical Transport Processes of Toroidal Plasmas; July 1995

NIFS-365 K. Itoh, S.-I. Itoh, A. Fukuyama and M. Yagi,
On the Minimum Circulating Power of Steady State Tokamaks; July 1995

NIFS-366 K. Itoh and Sanae-I. Itoh,
The Role of Electric Field in Confinement; July 1995

NIFS-367 F. Xiao and T. Yabe,
A Rational Function Based Scheme for Solving Advection Equation; July 1995

NIFS-368 Y. Takeiri, O. Kaneko, Y. Oka, K. Tsumori, E. Asano, R. Akiyama, T. Kawamoto and T. Kuroda,
Multi-Beamlet Focusing of Intense Negative Ion Beams by Aperture Displacement Technique; Aug. 1995

NIFS-369 A. Ando, Y. Takeiri, O. Kaneko, Y. Oka, K. Tsumori, E. Asano, T. Kawamoto, R. Akiyama and T. Kuroda,
Experiments of an Intense H- Ion Beam Acceleration; Aug. 1995

NIFS-370 M. Sasao, A. Taniike, I. Nomura, M. Wada, H. Yamaoka and M. Sato,
Development of Diagnostic Beams for Alpha Particle Measurement on ITER; Aug. 1995

NIFS-371 S. Yamaguchi, J. Yamamoto and O. Motojima;
A New Cable -in conduit Conductor Magnet with Insulated Strands; Sep. 1995

NIFS-372 H. Miura,
Enstrophy Generation in a Shock-Dominated Turbulence; Sep. 1995

NIFS-373 M. Natsir, A. Sagara, K. Tsuzuki, B. Tsuchiya, Y. Hasegawa, O. Motojima,
Control of Discharge Conditions to Reduce Hydrogen Content in Low Z Films Produced with DC Glow; Sep. 1995

NIFS-374 K. Tsuzuki, M. Natsir, N. Inoue, A. Sagara, N. Noda, O. Motojima, T. Mochizuki, I. Fujita, T. Hino and T. Yamashina,
Behavior of Hydrogen Atoms in Boron Films during H_2 and He Glow Discharge and Thermal Desorption; Sep. 1995

NIFS-375 U. Stroth, M. Murakami, R.A. Dory, H. Yamada, S. Okamura, F. Sano and T. Obiki, *Energy Confinement Scaling from the International Stellarator Database*; Sep. 1995

NIFS-376 S. Bazdenkov, T. Sato, K. Watanabe and The Complexity Simulation Group, *Multi-Scale Semi-Ideal Magnetohydrodynamics of a Tokamak Plasma;* Sep. 1995

NIFS-377 J. Uramoto, *Extraction of Negative Pionlike Particles from a H2 or D2 Gas Discharge Plasma in Magnetic Field;* Sep. 1995

NIFS-378 K. Akaishi, *Theoretical Consideration for the Outgassing Characteristics of an Unbaked Vacuum System*; Oct. 1995

NIFS-379 H. Shimazu, S. Machida and M. Tanaka, *Macro-Particle Simulation of Collisionless Parallel Shocks*; Oct. 1995

NIFS-380 N. Kondo and Y. Kondoh, *Eigenfunction Spectrum Analysis for Self-organization in Dissipative Solitons;* Oct. 1995

NIFS-381 Y. Kondoh, M. Yoshizawa, A. Nakano and T. Yabe, *Self-organization of Two-dimensional Incompressible Viscous Flow in a Friction-free Box;* Oct. 1995

NIFS-382 Y.N. Nejoh and H. Sanuki, *The Effects of the Beam and Ion Temperatures on Ion-Acoustic Waves in an Electron Beam-Plasma System;* Oct. 1995

NIFS-383 K. Ichiguchi, O. Motojima, K. Yamazaki, N. Nakajima and M. Okamoto *Flexibility of LHD Configuration with Multi-Layer Helical Coils;* Nov. 1995

NIFS-384 D. Biskamp, E. Schwarz and J.F. Drake, *Two-dimensional Electron Magnetohydrodynamic Turbulence*; Nov. 1995

NIFS-385 H. Kitabata, T. Hayashi, T. Sato and Complexity Simulation Group, *Impulsive Nature in Collisional Driven Reconnection*; Nov. 1995

NIFS-386 Y. Katoh, T. Muroga, A. Kohyama, R.E. Stoller, C. Namba and O. Motojima, *Rate Theory Modeling of Defect Evolution under Cascade Damage Conditions:The Influence of Vacancy-type Cascade Remnants and Application to the Defect Production Chracterization by Microstructural Analysis;* Nov. 1995

NIFS-387 K. Araki, S. Yanase and J. Mizushima, *Symmetry Breaking by Differential Rotation and Saddle-node Bifurcation of the Thermal Convection in a Spherical Shell*; Dec. 1995

NIFS-388 V.D. Pustovitov,
Control of Pfirsch-Schlüter Current by External Poloidal Magnetic Field in Conventional Stellarators: Dec. 1995

NIFS-389 K. Akaishi,
On the Outgassing Rate Versus Time Characteristics in the Pump-down of an Unbaked Vacuum System; Dec. 1995

NIFS-390 K.N. Sato, S. Murakami, N. Nakajima, K. Itoh,
Possibility of Simulation Experiments for Fast Particle Physics in Large Helical Device (LHD); Dec. 1995

NIFS-391 W.X.Wang, M. Okamoto, N. Nakajima, S. Murakami and N. Ohyabu,
A Monte Carlo Simulation Model for the Steady-State Plasma in the Scrape-off Layer; Dec. 1995

NIFS-392 Shao-ping Zhu, R. Horiuchi, T. Sato and The Complexity Simulation Group,
Self-organization Process of a Magnetohydrodynamic Plasma in the Presence of Thermal Conduction; Dec. 1995

NIFS-393 M. Ozaki, T. Sato, R. Horiuchi and the Complexity Simulation Group
Electromagnetic Instability and Anomalous Resistivity in a Magnetic Neutral Sheet; Dec. 1995

NIFS-394 K. Itoh, S.-I Itoh, M. Yagi and A. Fukuyama,
Subcritical Excitation of Plasma Turbulence; Jan. 1996

NIFS-395 H. Sugama and M. Okamoto, W. Horton and M. Wakatani,
Transport Processes and Entropy Production in Toroidal Plasmas with Gyrokinetic Eletromagnetic Turbulence; Jan. 1996

NIFS-396 T. Kato, T. Fujiwara and Y. Hanaoka,
X-ray Spectral Analysis of Yohkoh BCS Data on Sep. 6 1992 Flares - Blue Shift Component and Ion Abundances -; Feb. 1996

NIFS-397 H. Kuramoto, N. Hiraki, S. Moriyama, K. Toi, K. Sato, K. Narihara, A. Ejiri, T. Seki and JIPP T-IIU Group,
Measurement of the Poloidal Magnetic Field Profile with High Time Resolution Zeeman Polarimeter in the JIPP T-IIU Tokamak; Feb. 1996

NIFS-398 J.F. Wang, T. Amano, Y. Ogawa, N. Inoue,
Simulation of Burning Plasma Dynamics in ITER; Feb. 1996

NIFS-399 K. Itoh, S-I. Itoh, A. Fukuyama and M. Yagi,
Theory of Self-Sustained Turbulence in Confined Plasmas; Feb. 1996

NIFS-400 J. Uramoto,
A Detection Method of Negative Pionlike Particles from a H2 Gas

Descharge Plasma; Feb. 1996

NIFS-401 K.Ida, J.Xu, K.N.Sato, H.Sakakita and JIPP TII-U group,
Fast Charge Exchange Spectroscopy Using a Fabry-Perot Spectrometer in the JIPP TII-U Tokamak; Feb. 1996

NIFS-402 T. Amano,
Passive Shut-Down of ITER Plasma by Be Evaporation; Feb. 1996

NIFS-403 K. Orito,
A New Variable Transformation Technique for the Nonlinear Drift Vortex; Feb. 1996

NIFS-404 T. Oike, K. Kitachi, S. Ohdachi, K. Toi, S. Sakakibara, S. Morita, T. Morisaki, H. Suzuki, S. Okamura, K. Matsuoka and CHS group;
Measurement of Magnetic Field Fluctuations near Plasma Edge with Movable Magnetic Probe Array in the CHS Heliotron/Torsatron; Mar. 1996

NIFS-405 S.K. Guharay, K. Tsumori, M. Hamabe, Y. Takeiri, O. Kaneko, T. Kuroda,
Simple Emittance Measurement of H- Beams from a Large Plasma Source; Mar. 1996

NIFS-406 M. Tanaka and D. Biskamp,
Symmetry-Breaking due to Parallel Electron Motion and Resultant Scaling in Collisionless Magnetic Reconnection; Mar. 1996

NIFS-407 K. Kitachi, T. Oike, S. Ohdachi, K. Toi, R. Akiyama, A. Ejiri, Y. Hamada, H.Kuramoto, K. Narihara, T. Seki and JIPP T-IIU Group,
Measurement of Magnetic Field Fluctuations within Last Closed Flux Surface with Movable Magnetic Probe Array in the JIPP T-IIU Tokamak; Mar. 1996

NIFS-408 K. Hirose, S. Saito and Yoshi.H. Ichikawa
Structure of Period-2 Step-1 Accelerator Island in Area Preserving Maps; Mar. 1996

NIFS-409 G.Y.Yu, M. Okamoto, H. Sanuki, T. Amano,
Effect of Plasma Inertia on Vertical Displacement Instability in Tokamaks; Mar. 1996

NIFS-410 T. Yamagishi,
Solution of Initial Value Problem of Gyro-Kinetic Equation; Mar. 1996

NIFS-411 K. Ida and N. Nakajima,
Comparison of Parallel Viscosity with Neoclassical Theory; Apr. 1996

NIFS-412 T. Ohkawa and H. Ohkawa,
Cuspher, A Combined Confinement System; Apr. 1996